Solid State Phenomena
ISSN: 1662-9779, Vol. 255, pp 331-337
doi:10.4028/www.scientific.net/SSP.255.331

Online: 2016-09-05

Oxidation of Si Surfaces: Effect of Ambient Air and Water Treatments on Surface Charge and Interface State Density

Heike Angermann[1, a *], Patrice Balamou[2,b], Wenjia Lu[1,c], Lars Korte[1,d], Caspar Leendertz[1,e], and Bert Stegemann[2,f]

[1]Institute of Silicon Photovoltaics, Helmholtz Center Berlin, Kekuléstr. 5, 12489 Berlin, Germany

[2]HTW Berlin - University of Applied Sciences Berlin, Wilhelminenhofstr. 75a, 12459 Berlin, Germany

[a]angermann@helmholtz-berlin.de, [b]patrice.balamou@gmail.com, [c]lu.wenjia@hotmail.com, [d]korte@helmholtz-berlin.de, [e]leendertz@gmail.com, [f]bert.stegemann@htw-berlin.de

Keywords: Silicon solar cell substrates, wet-chemical oxidation, ultra-thin oxide layer, surface photovoltage SPV, surface charge, interface state density, Effective Lifetime Analysis ELifAnT

Abstract. Surface sensitive methods, UV-VIS spectral ellipsometry (SE), surface photovoltage (SPV) measurements, and X-ray photoelectron spectroscopy (XPS) measurements were combined to investigate in detail the Si substrate oxidation and resulting interface electronic properties. Various wet-chemical oxidation methods utilizing hot deionized water with different HCl or Ozone content were optimized in order to prepare ultra-thin oxide layers with reproducible oxide thicknesses ($<d_{ox}>$ 0.3 to 3.5 nm), low values of interface state densities and well-defined interface charges. The simulation tool ELifAnT (Effective Lifetime Analysis Tool) was utilised to analyse experimental excess minority charge carrier density (Δn) dependent charge carrier lifetimes $\tau_{eff}(\Delta n)$, and to establish correlations between preparation induced interface charges Q_{it} and defect densities D_{it} on both p-and n-type substrates.

1. Introduction

The concomitance of oxygen and humidity causes the initial oxidation of silicon surfaces during all steps of electronic device manufacturing. In order to avoid un-stoichiometric mixed phases of native Si oxides (SiO_x) at wet-chemically treated interfaces, the native oxidation of Si substrates was thoroughly investigated as an undesirable side effect of wafer storage and water rinsing procedures [1]. On the other hand, the initial oxidation of Si surfaces and the preparation of ultra-thin silicon oxide layers in deionized water (DiW) or diluted solutions of ozone or HCl can be utilized to optimize surface morphology and surface electronic properties with respect to the subsequent processing steps. Numerous technological applications of ultra-thin oxide layers on Si substrates have been reported, e.g., to improve the surface wettability prior to inline doping and diffusion for improved emitter formation [2], as passivation interlayer on contacts [3,4] in n^+-SIPOS/p-silicon heterojunction solar cells [5], prior to the deposition of all-PECVD AlO_x/a-SiN_x passivation stacks [6] or in amorphous/crystalline a-Si:H/c-Si heterojunction solar cells [7].

Essential requirement for all applications is the reproducible preparation of uniform ultrathin oxide layers with a thickness of < 2 nm and interfaces with low densities of defect states and defined interface charges. Thus, the goal of this study is the development of simple and surface sensitive tools for controlling and monitoring the initial oxidation processes during Si solar cell manufacturing. The understanding of the related modification of surface electronic properties is considered as a precondition to achieve Si substrate conditioning by ultra-thin wet-chemical oxides with defined interface charge and low interface state densities.

2. Preparation and experimental methods

Initially H-terminated polished p- and n-type Si(100) and Si(111) substrates were exposed in (i) cleanroom air (25°C, humidity 50%), (ii) deionized water (DiW: dissolved oxygen concentration D.O.C.~ 8 ppm) at 80°C, and (iii) diluted HCl solutions (HCl : H_2O, 1:10, 1: 100 and 1:1000).

Simultaneous UV-VIS spectral ellipsometry (SE) [8], surface photovoltage (SPV) measurements, and x-ray photoelectron spectroscopy (XPS) measurements were performed to monitor the change of oxide coverage and of the electronic surface properties during the exposition times ranging from 5 min to 180 h in air, and from 5 min to 6 h in DiW solutions, respectively.

UV-VIS spectral ellipsometry (SE) measurements in the ultraviolet and visible (UV-VIS) spectral range (angles of incidence of 70°, 60° and 50° in the wavelength range of 250 nm to 800 nm) were carries out immediately after preparation and surface oxidation. Assuming appropriate models values for the surface micro-roughness $<d_r>$ and the thickness of the ultra-thin oxide $<d_{ox}>$, respectively, were calculated. The optical effect of a microscopically rough surface can be described accurately [9] by a Bruggeman effective medium [10] (EMA) layer. For microscopically rough wafers a two layer model was used consisting of bulk c-Si [11] and a Bruggeman EMA layer consisting of 50% bulk c-Si and 50% voids. Wafers with an ultra-thin oxide layer $<d_{ox}>$ were modeled by a layer of SiO_2 [12] on top of c-Si. Here, the data from the initially H-terminated sample before oxidation were used to include a small fraction of surface roughness $<d_r>$ remaining after the H-termination procedure.

X-ray Photoelectron spectroscopy (XPS), which is a well-established technique for obtaining quantitative information on the interface composition and stoichiometry by analysis of the chemical shift of the Si 2p core-level electrons [13] was applied to characterize the chemical properties of the SiO_x/Si interface.

Field-dependent SPV is a very surface sensitive method, measuring the surface photo voltage U_{ph} as a function of the external bias voltage as recently described in detail in [14] using a mica foil dielectric spacer. A laser diode (902 nm, 150 ns pulse length) was used as a light source. The photovoltage pulses, as shown in Fig. 3a, were recorded with a transient recorder (resolution time 5 ns). The determination of the interface state density $D_{it}(E)$ by a pulsed field modulated SPV method was first published in 1968 by Heilig [15]. To determine the interface state density $D_{it}(E)$ (see Fig. 3b) a varying electric field perpendicular to the surface was applied, which changes the surface potential Φ_s continuously as a function of the field voltage U_F. Due to screening effects the influence U_F on the surface potential Φ_s depends on the charge Q_{it} trapped in interface states.

The simulation tool ELifAnT is a semianalytical simulation model, implemented in Mathematica®, that calculates the c-Si band bending and recombination rates at a c-Si hetero-interface such as the a-Si:H/c-Si interface, or the SiO_2/c-Si interface investigated in the present study. Briefly, band bending is calculated based on charge neutrality between c-Si (charge Q_{cSi}), interface states (Q_{int}) and the charge in the film forming the heterojunction to the c-Si substrate (Q_f), i.e. SiO_2 in the present case:

$$Q_{cSi}(\Delta n, \psi) + Q_{int}(\Delta n, \psi) + Q_{fix}(\Delta n, \psi) = 0 \quad (1)$$

Here, ψ is the c-Si band bending. The charge in the space charge region $Q_{cSi}(\Delta n, \psi)$ is calculated following Girisch et al. [16]. For the interface defect charges $Q_{int}(\Delta n, \psi)$, a Gaussian distribution centred around c-Si midgap is assumed, while the charge in the film is assumed to be fixed at a level of $+2x10^{11}$ cm^{-2}, based on literature findings for thick SiO_2 films [17].

To calculate charge in interface defects $Q_{int}(\Delta n, \psi)$ the injection-/band bending dependent carrier concentrations at the surface are determined from the standard Shockley-Read-Hall equations, integrating across the energetic distribution of the defects and using the approximation of flat quasi-Fermi levels throughout the junction. Thus, solving Eq. (1) numerically for ψ, the band bending is obtained for different injection levels Δn. This yields the positions of the quasi-Fermi levels at the c-Si/SiO_2 interface, enabling to calculate the effective interface recombination rate $U_{int}(\Delta n)$ based on Sah and Shockley's model [18] and thus the effective interface recombination rate $S_{eff} = U_{int}/\Delta n$.

This is then combined with a calculation of the injection level dependent minority carrier lifetime τ_b, yielding an effective carrier lifetime $\tau_{eff}(\tau_b, S_{eff}, \Delta_n)$: For good interface passivation, $1/\tau_{eff} = 1/\tau_b + 2\,S_{eff}/W$, W being the wafer thickness.

Varying the interface defect parameters and the fixed charge in the SiO_2, these τ_{eff} curves can be fitted to experimental data obtained from photoconductance decay (PCD) measurements, which were carried out on a commercial Sinton WCT-100 setup. For the present study, we are mainly interested in extracting the c-Si/SiO_2 interfacial charge Q_{it} [cm^{-2}] from these fits.

3. Influence of substrate properties and preparation conditions on surface oxidation rate

The native oxidation of Si surfaces in ambient air at room temperature (RT) is a long-lasting process. As shown by our recently reported results, during an initial phase ranging from 2 to 48 hours, the appearance of the first monolayer of silicon oxide causes a strong increase of the interface states density $D_{it}(E)$ about two orders of magnitudes.

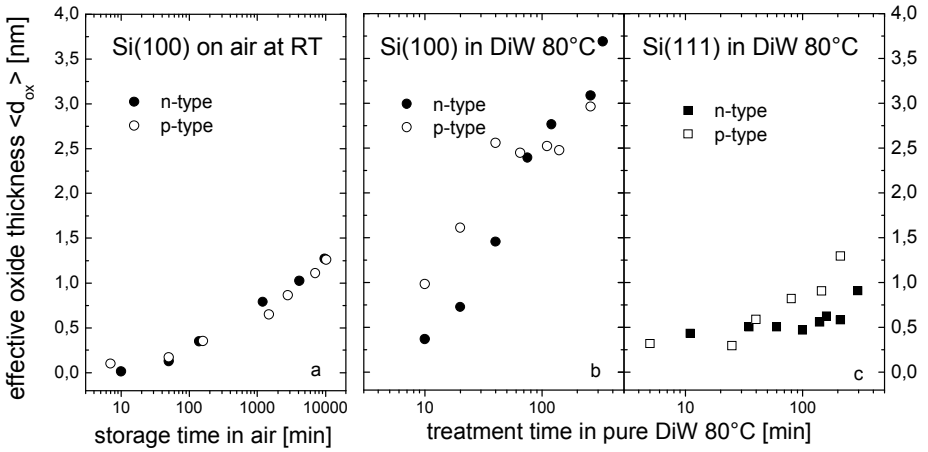

Fig. 1 Effective oxide thickness $<d_{ox}>$ on initially H-terminated p-and n-type Si(100) determined from UV-Vis SE measurements as function of immersion time in clean room air (a) and in DiW at 80°C (b and c).

The further native oxide growth is characterized by significant decrease of $D_{it}(E)$ and a continuous change of the surface charge Q_{it}. It takes at least 6 months and was found to be limited at oxide thicknesses $<d_{ox}>$ 1.5 … 3.0 nm [19]. A very fast oxide growth can be achieved at RT in diluted solutions of O_3 (3 … 50 ppm), but the rapid process causes high D_{it} values which in most cases are not suitable as passivation layer [2].

In order to optimize the wet-chemical oxide preparation without O_3 initially H-terminated p- and n-type Si(100) and Si(111) substrates were exposed in ultra-pure DiW at 80°C. In Fig. 1 $<d_{ox}>$ is shown as determined from SE measurements as a function of the immersion time in clean room air (a) and in DiW at 80°C (b and c).

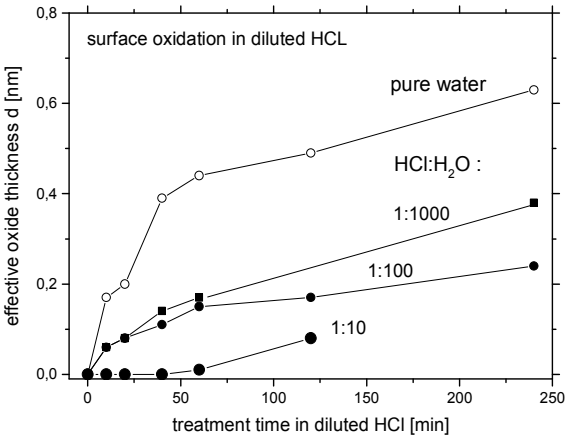

Fig. 2 Effective oxide thickness on initially H-terminated n-type Si(111) as function of immersion time in pure DiW at 80°C with increasing HCl content.

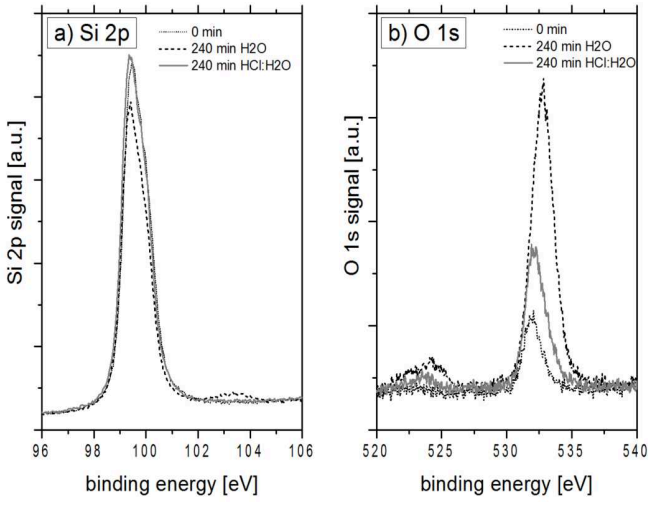

Fig. 3 XPS (a) Si 2p and (b) O 1s spectra of a Si(111) wafer, as cleaned, oxidized in H_2O and oxidized in HCl:H_2O.

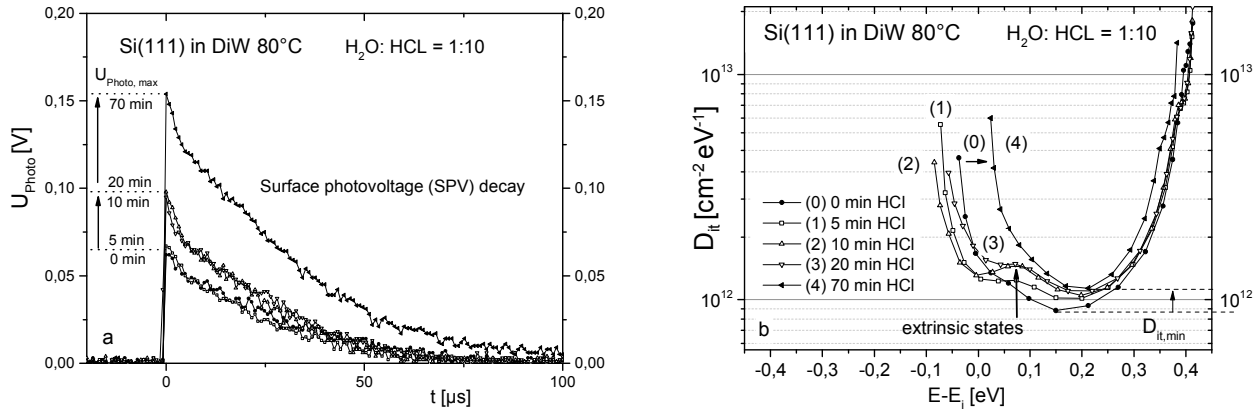

Fig. 4 SPV transients (a) measured without bias voltage and the determined $D_{it}(E)$ (b) on polished H-terminated n - Si surfaces after increasing exposition duration in $HCl:H_2O$ = 1: 10.

The growth rate in ultrapure water was found to be significantly higher compared to the native oxidation on air, and results in ultra-thin oxide layers of 1 … 3.5 nm thickness for Si(111) and Si(100), respectively [20]. The faster oxidation and higher final oxide thickness were obtained on Si(100), which can be explained by a higher O_2 diffusion rate due to greater Si atom distance compared to Si(111) [21].

In contrast to results obtained by ozone containing solutions [2], the addition of HCl results in a slower oxidation process of the Si surface and is superior to oxidation in pure H_2O with respect to a low $D_{it}(E)$. The influence of increasing HCl content on the evolution of effective oxide thickness on n-type Si(111) and on the XPS Si 2p and O 1s as function of immersion time in pure DiW at 80°C are shown in Fig. 2 and 3.

Typically, by means of XPS the amount of interfacial Si suboxides, i.e. oxidation states (i.e., Si^{1+}, Si^{2+}, Si^{3+}), that are present at the SiO_2/Si interface can be determined. However, in the present case of oxidation in $HCl:H_2O$ apparently just a very thin surface oxide is formed, yielding an XPS Si^{4+} 2p signal which was just above the detection limit. Thus, the amount of interfacial suboxides can be considered as negligible. Moreover, by comparison of the presented curves it is concluded that the presence of HCl decelerates the wet-chemical oxidation in hot water allowing for very precise oxide layer thickness control [22].

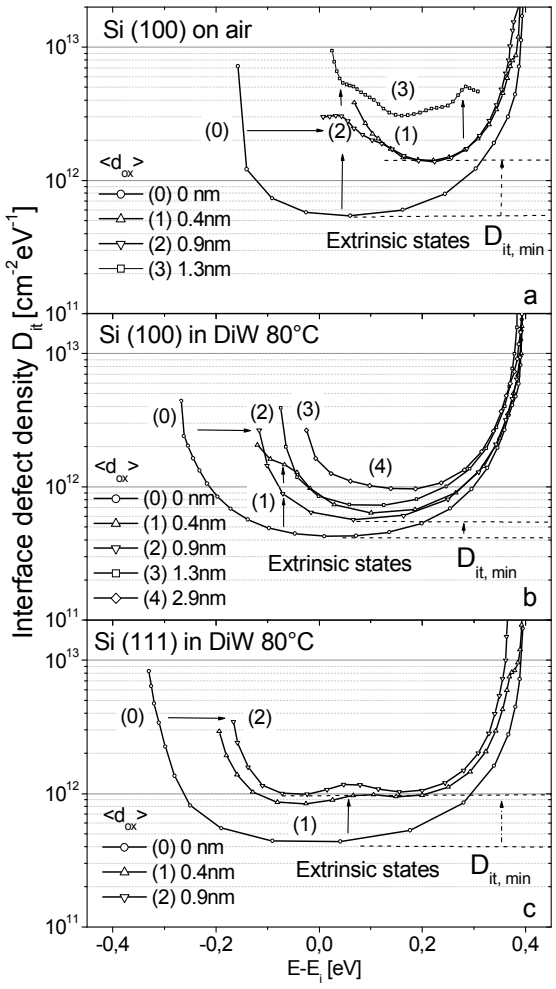

Fig. 5 $D_{it}(E)$ on initially H-terminated Si (curves 0) after preparation of ultra-thin oxide layers $<d_{ox}>$ 0.4 nm (curves 1), $<d_{ox}>$ 0,9 nm (curves 2), $<d_{ox}>$ 1,3 nm (curves 3) and $<d_{ox}>$ 2,9 nm (curve 4)

4. Evolution of interface state densities during silicon surface oxidation

In Fig. 4 are given the SPV transients (right) measured on n-type Si(111) substrates without bias voltage and the determined $D_{it}(E)$ (left) on initially H-terminated n -type Si after increasing exposition duration in $HCl:H_2O$ = 1:10. The wet-chemical oxidation of Si leads to an increase of $D_{it}(E)$ with immersion times and oxide thicknesses. Independent from the minimal value $D_{it,min}$ the appearance of extrinsic states - caused by dangling bond defects on Si atoms with lower stage of

oxidation - increases the density of rechargeable states in the lower part of the gap. As recently reported, this process was found to be strongly related to the O_3 or HCl content [20,23].

Fig. 5 shows for n-type Si substrates the effect of Si(100) and Si(111) surface orientation and oxidation conditions, which are investigated in detail by exposition in air at RT (Fig. 5a) and in pure DiW at 80° C (Fig. 5 b and c). During the initial phase of oxidation on the U- shaped $D_{it}(E)$ distribution of intrinsic states obtained on H-terminated surfaces (Fig. 5 a,b,c curves 0) different Gaussian distributed groups of extrinsic states additionally appears [24]. States in the lower part of the gap, related to defects on Si^{+1} were observed on Si(100) substrates (Fig. 5a,b, curves 1,2,3). The initial oxidation of Si(111) causes extrinsic states in the higher part of the gap (Fig. 5 c, curves 2,2) due to Si^{+2} defects [25]. On ultra-thin tunneling oxides ($<d_{ox}> \pm 0.9$ nm) prepared in DiW at 80° C (Fig. 5 b,c curves 2) significantly lower values of interface states in were observed, compared to native oxides grown on ambient air (Fig. 5a curve 2).

Lowest minimum values $D_{it,min} \leq 5 \cdot 10^{11} cm^{-2} eV^{-1}$ were achieved on Si(100), whereas on Si(111) least densities of rechargeable states in lower part of the gap were obtained.

5. Evaluation of surface charge on wet-chemically oxidized Si surfaces

To investigate the relation between the individual peaks in the D_{it} distributions of wet chemical oxides and the effective charge, the D_{it} values at energy levels of E-E_i = -0.1 eV and E-E_i = +0.2 eV in the Si band gap are extracted from $D_{it}(E)$ curves such as the ones depicted in Fig. 5. Furthermore, the ELifAnT tool was used to calculate the effective interface charges Q_{it} from TrPCD carrier lifetime data obtained from symmetrical samples with the same oxide passivation. The two D_{it} values and the effective interface charge Q_{it} are plotted as functions of the oxide thickness in Fig. 6. To see the correlation more clearly, the range of the tunneling interlayer thickness is here broadened to 0-2 nm.

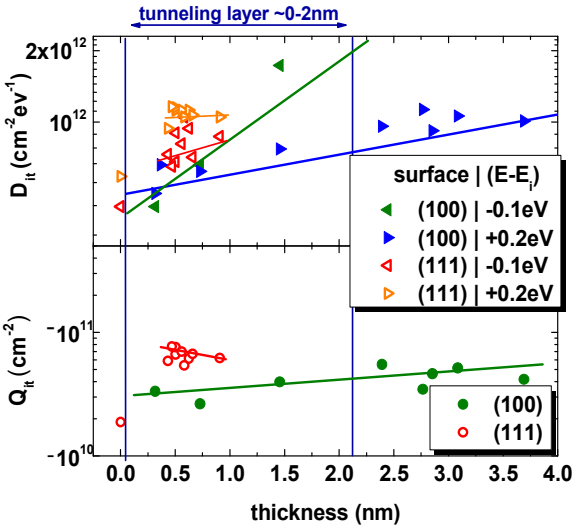

Fig. 6 Effective interface charge Q_{it} for oxides on n type Si(100) and Si(111) as functions of $<d_{ox}>$. The lines are guides for the eye.

It is apparent from Fig. 6 that no pronounced correlation exists between Q_{it} and D_{it}. A detailed understanding and a simulation is complicated because the D_{it} values do not increase over the whole band gap and separate defect peaks at different energy positions are present, as can be seen in Fig. 5 (middle panel). Note that the situation is different from what we find in native oxide growth in c-Si (data not shown): An increase of D_{it} from ~0.5×10^{12} $cm^{-2}eV^{-1}$ to ~3×10^{12} $cm^{-2}eV^{-1}$ during native oxide growth is accompanied by a change of Q_{it} from ~4×10^{10} cm^{-2} to -4×10^{10} cm^{-2}, i.e. even including a sign reversal of the charge.

In order to assess their suitability as tunnel layers, we discuss the properties of the best (low $D_{it,min}$) chemically grown oxides with thicknesses < 1nm: For the oxide on (100) oriented (n)c-Si, an oxide thickness of 0.7nm is reached after 20 minutes of oxidation, with a D_{it} of 5.6×10^{11} $cm^{-2}eV^{-1}$. Q_{it} = -2.6×10^{10} cm^{-2} is rather low for this surface orientation. For the chemically grown oxides on (111) n-type c-Si, after 100 min oxidation we find an oxide thickness of 0.5 nm, with a slightly higher $D_{it,min}$ value of 7.6×10^{11} $cm^{-2}eV^{-1}$. However, in this case the fixed charge is increased to -7.7×10^{10} cm^{-2}, which is beneficial if this oxide is used as an tunnel layer in a hole collecting contact, e.g. in a (p)a-Si:H/SiO_2/(n)c-Si emitter structure.

It should be noted, that for the usual random pyramid surface texture used in monocrystalline silicon solar cells, the (111) surface is the technologically relevant one, since the facets of the random pyramids exhibit this surface orientation.

6. Summary

By simultaneous determination of several oxide parameters, i.e. oxide coverage, interface charges Q_{it} and density of interface states D_{it}, correlations were established between the substrate properties, the process parameters, the kinetics of oxide formation and the evolving surface electronic properties. The detailed understanding of the initial oxidation processes could be used to optimize wafer storage, cleaning and rinsing processes in order to avoid contaminations with undesirable un-stoichiometric native oxides. It was shown that ultra-thin oxide layers ($<d_{ox}>$ 0.3 … 3.5 nm) with low interface state densities $D_{it,min} \sim 5\ldots 9 \cdot 10^{11} cm^{-2} eV^{-1}$ and well defined surface charges can be prepared by wet-chemical oxidation in DiW at 80 ° C.

The addition of HCl lowers the oxidation rate, however, a short oxidation in presence of chlorine (high dilution preferable i.e. 1:100 … 1:1000) and an immediate oxide removal offers the possibility to eliminate further metal contaminations and to improve the electronic interface properties [22]. For the chemically grown oxides on the technologically relevant (111) n-type c-Si surface, a 0.5nm tunnel oxide can be grown within 100 min, yielding a $D_{it,min}$ of $7.6 \cdot 10^{11}$ $cm^{-2}eV^{-1}$ and a fixed charge Q_{it} of $-7.7 \cdot 10^{10}$ cm^{-2}. This charge can support the band bending if the oxide is used as a tunnel layer in a hole collecting contact, e.g. in a (p)a-Si:H/SiO_2/(n)c-Si emitter structure.

Application of this results e.g. in the realization of tunnel oxide-based solar cell concepts allows for the selection of the proper oxidation techniques to obtain high-quality SiO_2/Si interface and, thus, contributes to further improvements of the conversion efficiency.

References

[1] D. Gräf, M. Grundner, R. Schulz, J. Vac. Sci. Technol. A7 (1989) 808.
[2] K. Wolke, Ch. Gottschalk, A. Moldovan, A. Oltersdorf , H. Angermann, In: H. Ossenbrink, [u.a.] [Eds.] : 26th European Photovoltaic Solar Energy Conference 5 - 9 September, Hamburg, Germany. München: WIP, 2011.
[3] A. Moldovan, F. Feldmann, M. Zimmer, J. Rentsch, J. Benick, and M. Hermle, *Solar Energy Materials and Solar Cells*, SI: Proceedings of the 5th International Conference on Crystalline Silicon Photovoltaics (SiliconPV 2015), 142 (November 2015): 123–27.
[4] U. Römer, R. Peibst, T. Ohrdes, B. Lim, J. Krügener, E. Bugiel, T. Wietler, and R. Brendel. *Solar Energy Materials and Solar Cells*, SI: SiliconPV 2014, 131 (Dezember 2014): 85–91. doi:10.1016/j.solmat.2014.06.003
[5] W. Füssel, H. Eschrich, L. Elstner, M. Schmidt, N.D. Sinh, W. Henrion, H. Angermann, H. Flietner, R. Henschel, G. Krageler, G. Willeke, Proc. 13 Europ. PV Solar Energy Conf., Stepens Ed. (1995) 45.
[6] A. Laades, H. Angermann, H.-P. Sperlich, U. Stürzebecher, C. Álvarez, M. Bähr, A. Lawerenz, Solid State Phenomena 195 (2013) 310.
[7] R. Varache, H. Angermann, M.-E. Farret, J.P. Kleider, L. Korte, Proc. of the 27th EU PVSEC - European Photovoltaic Solar Energy Conference and Exhibition Frankfurt / Main, Germany, (2012) 1582 – 1585.
[8] W. Henrion, M. Rebien, H. Angermann, A. Roeseler, Appl. Surf. Sci. 202 (2002) 199.
[9] D.E. Aspnes, Phys. Rev. B41 (15) (1990) 10334.
[10] D.A.G. Bruggeman, Ann. Phys. (Leipzig) 24 (1935) 636.
[11] T. Yasuda and D.E. Aspnes , Appl. Opt. 33 (1994) 7435.
[12] B. Brixner, in: E.D. Palik, ed., Handbook of Optical Constants of Solids, (Academic Press, New York 1985), 759.
[13] B. Stegemann, D. Sixtensson, T. Lussky, A. Schoepke, I. Didschuns, B. Rech, M. Schmidt, Nanotechnology 19 (2008) 424020.
[14] H. Angermann, Anal. Bioanal. Chem. 374 (2002) 676.
[15] K. Heilig, Experimentelle Technik der Physik 14 (1968) 135.
[16] R. Girisch, R. Mertens, and R. D. Keersmaecker, IEEE Trans. Electron Devices 35(2) (1988) 203–222.

[17] Aberle, A. G., Glunz, S. & Warta, W. J. Appl. Phys. 71, (1992) 4422.
[18] C. T. Sah and W. Shockley, Phys. Rev. 109(4) (1958) 1103.
[19] H. Angermann, W. Henrion, M. Rebien, A. Röseler, Solid State Phenomena Vol. 92 (2003) 179-182.
[20] Lu, W.; Leendertz, C.; Korte, L.; Töfflinger, J.A.; Angermann, H.: Energy Procedia 55 (2014) 805-812.
[21] H. Angermann, W. Henrion, A. Röseler, M. Rebien, Materials Science and Engineering B73 (2000) 178.
[22] P. Balamou, H. Angermann, B. Stegemann, In: Photovoltaic Specialist Conference (PVSC) New Orleans,LA, 2015 IEEE 42nd. IEEE Journal of Photovoltaics 5,(2015) 1-5.
[23] Angermann, Heike; Wolke, Klaus; Gottschalk, Christiane; Moldovan, Ana; Roczen, Maurizio; Fittkau, Jens; Zimmer, Martin; Rentsch, Jochen: Apl. Surf. Scie. 258 (2012) 8387-8396.
[24] J. P. Campbell, P. M. Lenahan, Appl. Phys. Lett. 80, (2002) 1945.
[25] T. Hattori, Critical Reviews in Solid State and Materials Science 20 (4) (1995) 339.